World Scientific Research Journal Volume 11 Issue 12, 2025
ISSN: 2472-3703 DOI: 10.6911/WSRJ.202512_11(12).0003

Semiconductor Physics, Simulation Methods and Devices

Shancheng Liu, Yuan Xiang, Bowen Chen, Zhengran Zhao

Shanghai United International School (Qingpu Campas), Qingpu, Shanghai, 201704, China

Abstract

Semiconductors are materials that are between conductors and insulators. Because of their special electrical properties, they are widely used in modern electronics. This review first outlines the basic ideas of semiconductor, and how intrinsic semiconductors (pure material like silicon) can be changed into extrinsic semiconductors (p-type or n-type) semiconductors by doping and explains how temperature affect the carrier concentration and conductivity of extrinsic semiconductor. We then introduce a modelling perspective by using a first-principles calculation tool, CASTEP, to perform basic simulations on the electronic properties of semiconductor materials. Finally, we summarize key application of semiconductors in solar cell.

Keywords

Semiconductor physics; Doping effects; Fiest-principles calculation; CASTEP simulation; Solar cell application.

1. INTRODUCTION

Since the invention of the transistor in 1948, semiconductor technology has experienced rapid development. [1] Especially in the past 20 years, whether it is the chips in smartphones and autonomous vehicles, the GPUs providing computational power, the solar panels on space probes, or computer displays—these seemingly diverse devices all rely on one key material: the semiconductor. Its widespread application across various fields stems from its unique electrical properties. Unlike metals, which conduct electricity freely, or insulators, which block current completely, semiconductor's conductivity can be precisely controlled. This controllability has allowed engineers to make circuits increasingly smaller and more refined, driving the explosive growth of electronic devices over just a few decades.

To understand this unique property, first need to understand the concept of band structure and band gap, which determine whether a semiconductor material can conduct electricity. For an intrinsic semiconductor, conductivity arises when electrons are excited from the valence band to the conduction band. By introducing impurity atoms such as boron or phosphorus into the crystal lattice, we can transform an intrinsic semiconductor into either a p-type or n-type material, and a pn junction can be formed at the interface between the two. [2] This structure underpins the operation of diodes, transistors, and even solar cells. Chapter 5 will systematically explain the principle of solar cell.

However, experimental methods are not the only way to understand semiconductors. With the advancement of computational physics, quantum mechanical calculations based on first-principles methods have become another way to investigate band structures, density of states, and doping effects. They have been proven to accurately predict various properties of materials, including mechanical and electronic properties

ISSN: 2472-3703 DOI: 10.6911/WSRJ.202512_11(12).0003

2. PRINCIPLE OF SEMICONDUCTOR

2.1. Intrinsic Semiconductor

Since the late 1960s, silicon has been used as the matrix for integrated sensors. High-purity silicon is an intrinsic semiconductor. In terms of band structure, the valence band is completely filled with electrons, while the conduction band is empty. For conduction to occur, electrons must overcome the energy gap between the conduction band and the valence band—known as the band gap. At room temperature, some electrons are thermally excited into the conduction band, leaving behind holes in the valence band.

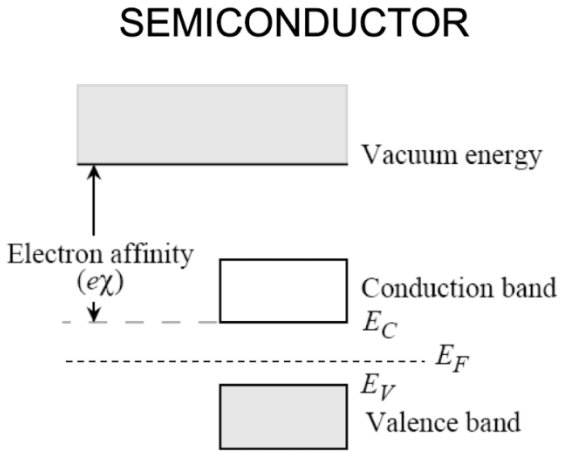

Figure 1. Band structure of pure Si

The number of electrons n excited into the conduction band can be calculated using the Fermi-Dirac distribution f(E) and the density of states n(E).

$$n = \int f(E)n(E)dE$$

Where f(E) is probability of electron occupation given by Fermi-Dirac distribution and n(E) is the density of state. [3]

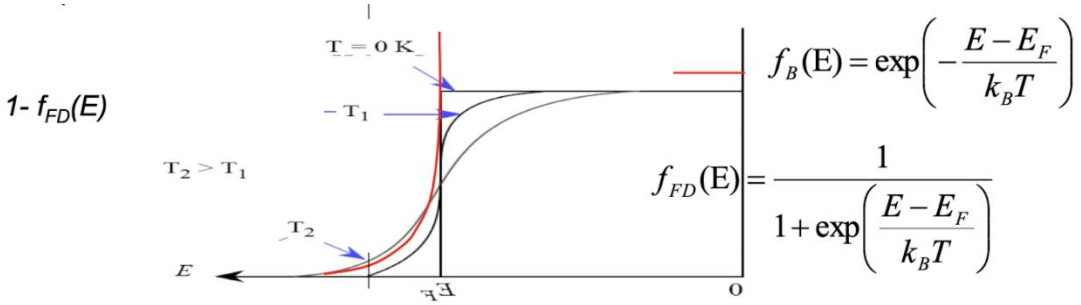

Figure 2. Fermi-Dirac distribution and Boltzmann distribution

Provided $E_f - E_v$ exceeds roughly $2K_BT$, the f(E) in the valance band can be approximated by the Boltzmann distribution.

For three dimension crystal, density of state in valance band is:

$$n(E) = \frac{1}{2\pi^2}\left(\frac{2}{\hbar^2}\right)^{3/2} m_e^{*2/3}(E - E_c)^{1/2}$$

Where E_c is the energy of conduction band, and m_e^* is the effective mass. Substituting into formula of n and get:

ISSN: 2472-3703 DOI: 10.6911/WSRJ.202512_11(12).0003

$$n = N_c \exp\left(\frac{-(E_c - E_f)}{k_B T}\right)$$

And $N_c = 2\left(\frac{2\pi m_e^* k_B T}{h^2}\right)^{3/2}$

For intrinsic semiconductor, the number of electrons in conduction band is and number of holes in the valance band are the same. Due to the expression of n, the carrier density rises as $T^{3/2}$, which means higher temperature, higher carrier density, higher conductivity.

2.2. Extrinsic Semiconductor

In an intrinsic material, adding a small amount of impurities can significantly change the properties of the semiconductor. For silicon, it is common to dope with pentavalent impurities such as arsenic (As) or trivalent elements such as boron (B). Arsenic has one more valence electron than silicon, so if an As atom is introduced into the crystal, there will be one extra electron (figure 3). These extra electrons produced by doping are called donors. In the energy level diagram, the donor energy level is very close to the conduction band, which means band gap is much smaller compared with pure Si material (figure 4). So electrons need less energy to be excited into the conduction band and conduct electricity. This type of material, where electrons are the majority carriers, is called n-type semiconductor

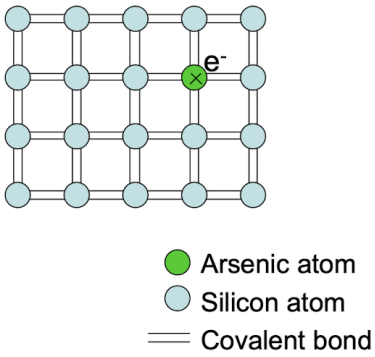

Figure 3. Crystal structure of As doped silicon

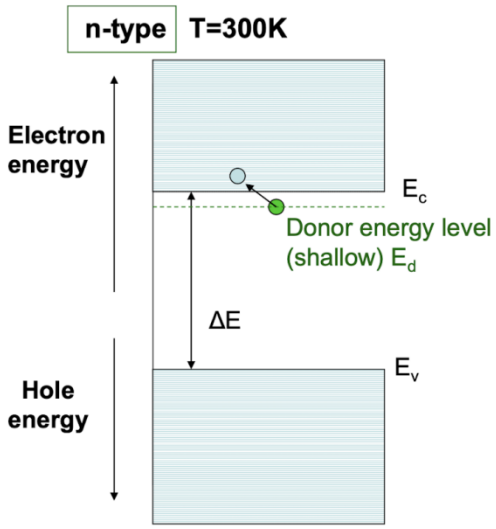

Figure 4. Band structure

For silicon, if it is doped with a trivalent element such as boron (B), it has one fewer valence electron than silicon. When a B atom enters the crystal lattice, it leaves an “empty spot” in the covalent bonds with surrounding silicon atoms, known as a hole (figure 5). In the energy level diagram, this corresponds to an acceptor energy level located very close to the valence band (figure 6). As a result, electrons in the valence band need only a small amount of energy to jump to the acceptor level, leaving behind mobile holes that can conduct electricity. This type of semiconductor, where holes are the majority carriers, is called p-type semiconductor.

ISSN: 2472-3703 DOI: 10.6911/WSRJ.202512_11(12).0003

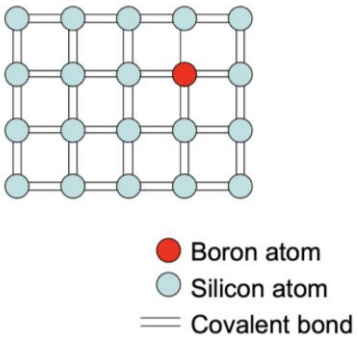

Figure 5. Crystal structure of As doped silicon

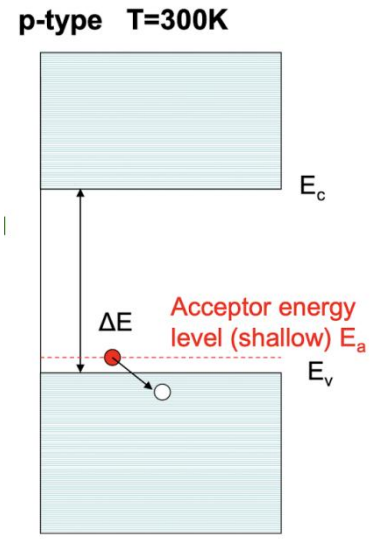

Figure 6. Band structure

For p type semiconductor, the majority carrier is holes (accepters), so the expression for number of carriers p:

$$p = N_a = N_v \exp\left(\frac{-(E_f - E_v)}{k_B T}\right)$$

Similarly, for n type semiconductor, the majority carrier is electrons (donors), so the expression for number of carriers n:

$$n = N_d = N_c \exp\left(\frac{-(E_c - E_f)}{k_B T}\right)$$

The effect of temperature on carrier concentration in a doped semiconductor is clearly illustrated in figure 7. At low temperatures, the material is in the freeze-out range, donors or acceptors are only partially ionized because the thermal energy is extremely low. Although band gap is very small for extrinsic semiconductor, there is still not enough energy to excite electrons to higher energy levels. Most dopant atoms remain neutral, so the number of free electrons or holes is far below the doping level. When temperature increases, thermal energy increases, leading to complete ionization. The material enters the saturation range, where the majority carrier concentration is approximately equal to the donor or acceptor concentration, remaining nearly constant with temperature. At high temperatures, thermally generated electron–hole pairs dominate, and the semiconductor enters the intrinsic range. The carrier concentration increases exponentially with temperature, far exceeding the contribution from doping. In the plot, higher doping levels produce a higher level in the saturation range, but the sharp rise in the intrinsic range is almost identical across samples, as it is determined by the intrinsic band gap of the material.

ISSN: 2472-3703 DOI: 10.6911/WSRJ.202512_11(12).0003

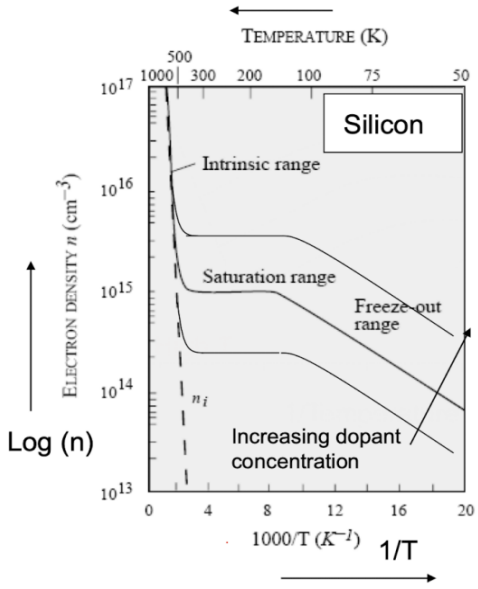

Figure 7. Electron density vs temperature

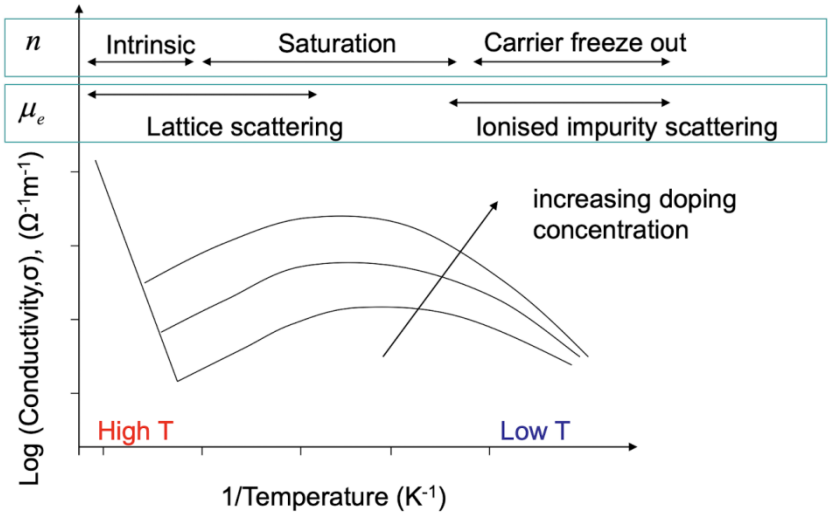

Figure 8. Conductivity vs temperature

Temperature affects not only the carrier concentration but also the carrier mobility, which strongly influences the electrical conductivity σ of semiconductor. Figure 8 shows the effect of temperature on conductivity in a doped semiconductor. At low temperatures, in the freeze-out range, there is not enough energy to activate donor or acceptor atoms, leading to low carrier concentration. At the same time, mobility is limited by ionized impurity scattering, so conductivity drops as temperature decreases. As temperature increases and reaches saturation region, dopants are almost fully ionized and carrier concentration remains constant, so conductivity increases. Mobility is now dominated by lattice scattering, which worsens with higher temperatures. So if keep increasing temperature, conductivity will decrease. At even higher temperatures, in the intrinsic range, thermally generated electron–hole pairs increase exponentially. Although mobility continues to decrease, the rapid growth in carrier concentration dominates, making conductivity rise sharply against temperature. Increasing the doping level shifts the conductivity in the saturation range upward, while the overall trends in each temperature regime remain the same.

ISSN: 2472-3703 DOI: 10.6911/WSRJ.202512_11(12).0003

2.3. PN Junction

PN junction is formed when a p-type semiconductor and a n-type semiconductor are brought into contact. The majority carriers in p region are holes, while in n region the majority carriers are electrons. Because of the difference in electron concentration, electrons in n region will diffuse to p region and combine with the holes near the PN junction. This leaves behind a region depleted of mobile charge-the depletion region, show in figure 9 [4].

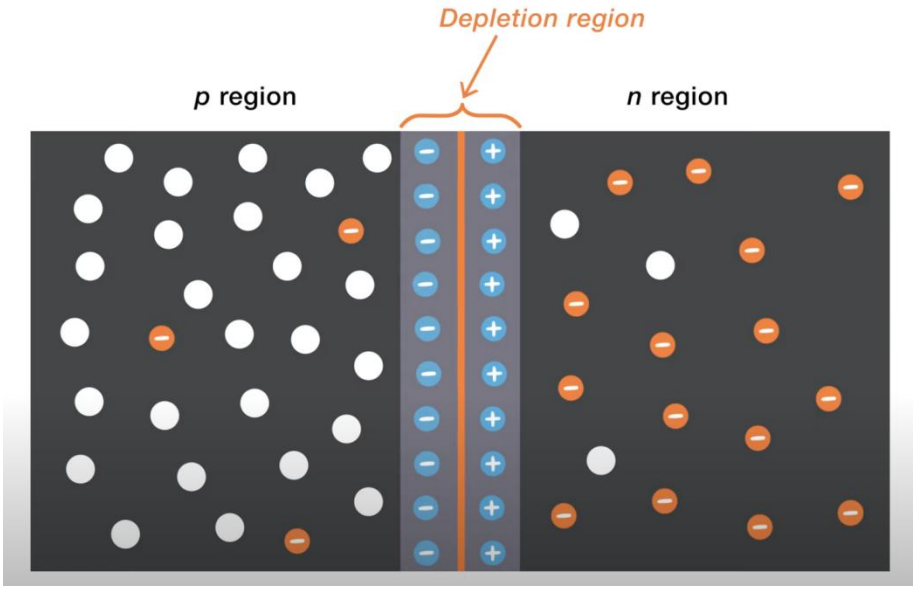

Figure 9. Depletion region

In the depletion region of a PN junction, positive charge on n side and negative charge on p side create an internal electric field pointing from the n side to the p side. This electric field is associated with a built-in potential V_{bi}, which opposes any further diffusion of electrons from the n region into the p region. As a result, at thermal equilibrium, the net electron diffusion from n to p is balanced by the drift motion of electrons in the opposite direction, driven by the electric field. The net current is just the sum of diffusion current and drift current.

$$I_{diffusion} = eD_e \frac{dn}{dx}$$

$$I_{drift} = en\mu_e \xi$$

$$I_e = I_{diffusion} + I_{drift} = e(D_e \frac{dn}{dx} + \mu_e \xi)$$

Where D_e is the diffusion coefficien of electront (Fick's fiest law)

μ_e is the mobility of electron

ξ is the internal electric field

3. ATOMIC MODELLING USING DFT

3.1. DFT Basic Ideas

In recent years, quantum mechanical calculations based on First-principles methods have played an important role in the field of materials science. They have been proven to accurately predict various properties of materials, including mechanical and electronic properties. Among

ISSN: 2472-3703 DOI: 10.6911/WSRJ.202512_11(12).0003

these methods, density functional theory (DFT) stands out as one of the most advanced approaches because of its high accuracy and computational efficiency.

In DFT, the total energy is expressed as the sum of four components: the kinetic energy of non-interacting electrons, the repulsion between electrons (Hartree energy), the attractive potential energy between electrons and nuclei, and the exchange-correlation energy. All the terms are function of electron density except the exchange-correlation energy, which accounts for all the complex quantum effects not considered by the other terms [5].

The Kohn-Sham equations provide a practical way to calculate the electron density by solving a set of single-electron equations. Under the condition of electrons do not interact with each other, coulomb potential $V_n(r)$ and Hartree potential $V_H(r)$ can be calculated, the only unknown term is the exchange correlation potential.

$$\left[-\frac{\nabla^2}{2} + V_n(r) + V_H(r) + V_{xc}(r)\right] \emptyset_i = \in_i \emptyset_i(r)$$

The Local Density Approximation (LDA) [6] is a widely used method to approximate the exchange-correlation energy E_{xc} and exchange-correlation potential V_{xc}. LDA assumes that the exchange-correlation energy density at a point depends only on the local electron density, and the energy density is the same as that of a homogeneous electron gas with the same density.

$$E_{xc}[n] = \int \rho(r) \in_{xc} (\rho(r)) dr$$

$\rho(r)$ is the electron density at a point, and $\in_{xc} (\rho(r))$ is the exchange-correlation energy density derived from the homogeneous electron gas model.

By substituting the electron density and exchange-correlation energy obtained from the Kohn-Sham equations into the total energy functional, the system's ground-state total energy can be calculated.

When running DFT on a computer, the self-consistent field method can be used, which solves the Kohn-Sham equations to obtain the ground-state electron density and total energy. First, an initial guess is made for the electron density or wavefunction. Based on this electron density, the Hamiltonian is constructed, which includes the kinetic energy term, the electrostatic potential from atomic nuclei, the Hartree potential for electron-electron interactions, and an exchange-correlation potential. The Kohn-Sham equations are then solved to obtain new wavefunctions and energy eigenvalues, which are used to update the electron density. The total energy and changes in density are calculated. If the convergence criteria are not met, the updated density is used to repeat the above process. Once convergence is achieved, the ground-state electron density, total energy, and other physical properties are output.

3.2. Case Study

In this section, several case studies are presented to illustrate the application of density functional theory (DFT) in modelling the electronic properties of semiconductors. The selected materials — silicon (Si), tin monosulfide (SnS), and tin disulfide (SnS_2) are chosen not only for their electronic characteristics, but also for their relevance in energy technologies.

ISSN: 2472-3703 DOI: 10.6911/WSRJ.202512_11(12).0003

(1) Si

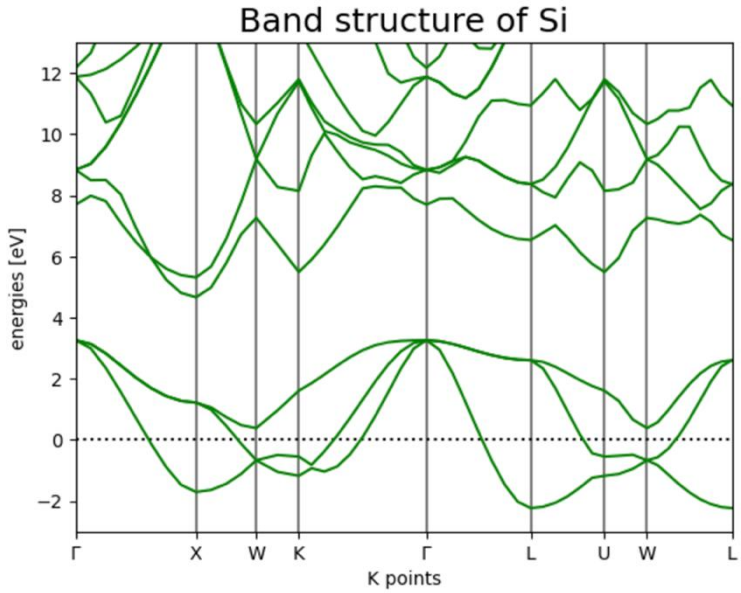

Figure 10. Si band structure

Figure 10 shows the band structure of silicon. A clear band gap is observed between the valence band and the conduction band. The conduction band minimum is located near the L point, while the valence band maximum is near the Γ point, indicating an indirect band gap of approximately 1.1 eV. This value is close to the experimental value (~1.12 eV) and lies near the optimal range for photovoltaic energy conversion, which explains why silicon remains the dominant absorber material in commercial solar cells [7].

(2) SnS

The partial density of state and band structure of SnS are shown in figure 11 and 12.

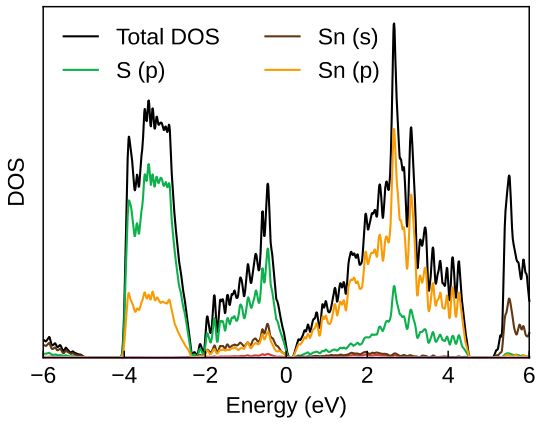

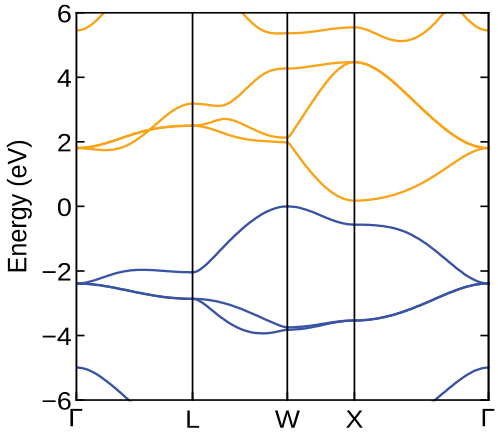

Figure 11. PDOS of SnS

Figure 12. Band structure of SnS

According to the band structure, the top of the valence band and the bottom of the conduction band are located at different k-points, indicating that SnS is an indirect semiconductor. The top of the valence band is near the W point at 0.083 Har, while the bottom of the conduction band is near the X point at 0.089 Har, resulting in a band gap of 0.15eV. Compared to the experimental value of 0.17 eV [8], the band gap is 10.76% lower, which is a common issue in DFT simulations. According to Figure 11, the valence band is mainly contributed by the S p orbitals, while the conduction band is mainly contributed by the Sn p orbitals. Mulliken charge analysis shows that the S 3p orbitals have a higher electron count of 4.63 e, while the Sn 5p orbitals have a lower electron occupancy of around 1.53 e. Therefore, the S 3p orbitals are the main component of the

ISSN: 2472-3703 DOI: 10.6911/WSRJ.202512_11(12).0003

valence band, which is consistent with the PDOS plot. In Figure 11, the DOS lines are not smooth because the Gaussian value was set to 0.05 instead of 0.1 when plotting with Sumo. This adjustment was made because DFT tends to underestimate the band gap size. If Gaussian = 0.1 were used, it would be very difficult to see the band gap in the PDOS plot.

(3) SnS2

The partial density of state and band structure of SnS2 are shown in figure 13 and 14.

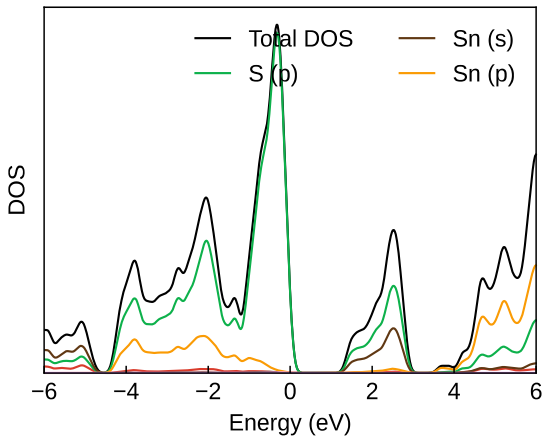

Figure 13. PDOS of SnS2

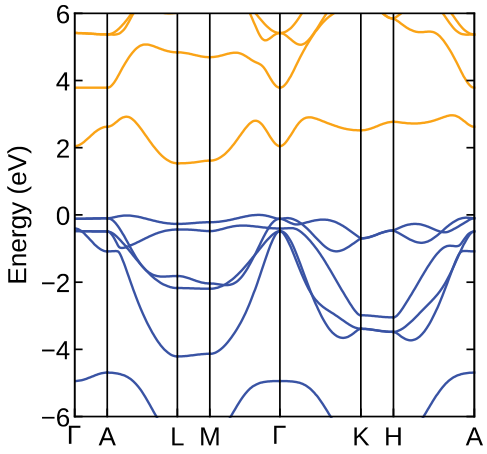

Figure 14. Band structure of SnS2

SnS_2 has an indirect band gap. From the band structure, the top of the valence band is between the M point and the Γ point, at 0.04834950 Har, while the bottom of the conduction band is near the L point, at 0.10478080 Har, leading to a band gap of 1.5236 eV, which is slightly higher than the experimental value of 1.51 eV [7], differing from the usual trend. A possible reason for this difference could be small errors in reading the valence and conduction band data. PDOS analysis shows that the valence band is mainly formed by S-p orbitals. In the conduction band, there are two subregions with an energy difference of about 1 eV. In the first subregion, which is close to the Fermi level, the DOS is mainly contributed by a mix of Sn-s and S-p orbitals. In the second subregion, the main contribution comes from the p orbitals of Sn and S atoms.

4. APPLICATION: SOLAR CELL

Solar cells are an important application of semiconductors which based on the photovoltaic effect. When the energy of an incident light is greater than the band gap, it can excite an electron from the valence band to the conduction band, generating an electron–hole pair. Photons with energy lower than the band gap cannot be absorbed, while the excess energy of photons above the band gap is converted into heat. As we discussed in Chapter 3, an electric field exists in the PN junction, which drives photo-generated electrons toward the n side and holes toward the p side. Subsequently, the carriers are collected in the external circuit, forming a photocurrent J_{ph}. Figure 15 clearly shows this process.

ISSN: 2472-3703 DOI: 10.6911/WSRJ.202512_11(12).0003

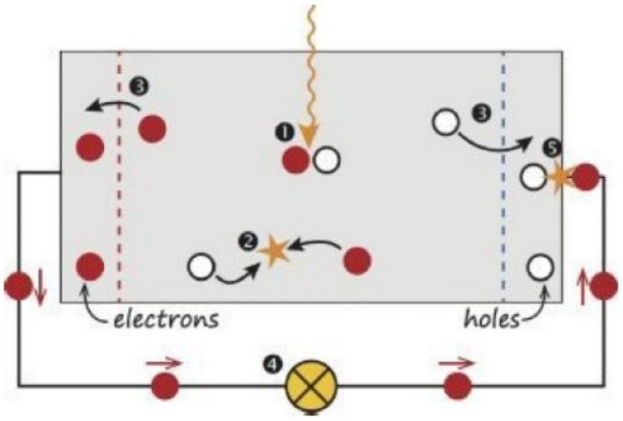

Figure 15. solar cell

The expression for net current J is:

$$J = J_{ph} - J_0[\exp\left(\frac{qV}{nk_BT}\right) - 1]$$

Where J_0 is the dark current

The energy difference between the quasi-Fermi energy level of electrons (ε_{Fn}) and holes (ε_{Fh}) determines the open-circuit voltage:

$$V = \frac{\varepsilon_{Fn} - \varepsilon_{Fh}}{e}$$

Therefore, selecting a semiconductor material with an appropriate band gap is very important. If the band gap is large, open circuit voltage will be large, but a large number of photons with energy below the band gap cannot be absorbed, which leads to small current; If the band gap is small, a large range of phonons can be absorbed, but the open circuit voltage will be very small. Figure 16 shows how current density varies against band gap and figure 17 shows how maximum power changes with bandgap.

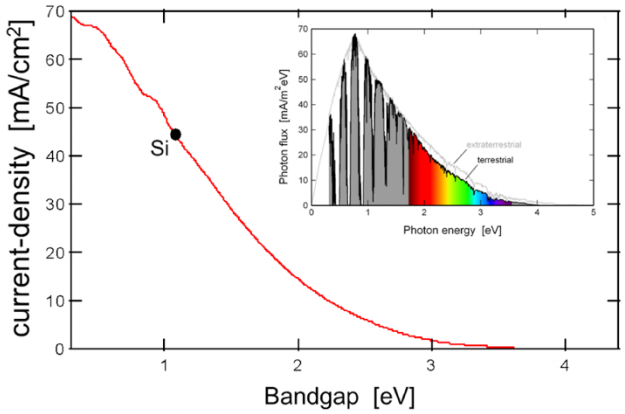

Figure 16. Current density vs bandgap

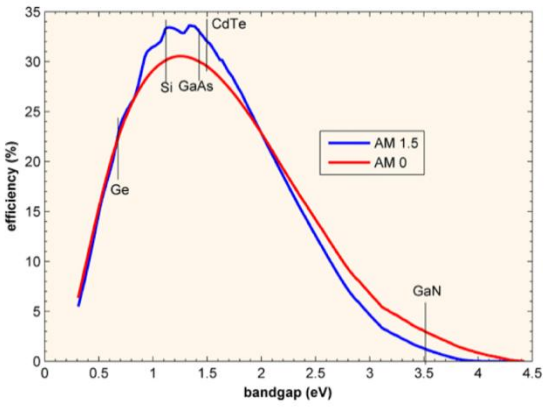

Figure 17. Efficiency vs bandgap

From Chapter 4, we obtained a band gap of approximately 1.11 eV for Si. This band gap lies in a relatively ideal range, enabling a high open-circuit voltage. However, due to its weak optical absorption, crystalline silicon solar cells normally have thickness around the order of hundreds of micrometers, combined with anti-reflection coatings and surface passivation, to increase J_{ph} and reduce J_0, thereby improving the net current. Silicon solar cells exhibit an efficiency in the range of 22–25%, and currently, approximately 80% of all solar cells are using silicon [7].

ISSN: 2472-3703 DOI: 10.6911/WSRJ.202512_11(12).0003

"SnS solar cell has emerged as a promising alternative to traditional photovoltaic technologies among various solar cells." [9] SnS has a smaller bandgap (0.15 eV in our F43m phase calculation, other phases are closer to 1.3 eV and more suitable for photovoltaics). Its high absorption coefficient and non-toxic composition make it suitable for thin-film cells, though voltage output is limited by the small bandgap, requiring GLAD technique and CZTSSe layer to improve efficiency [9].

REFERENCES

[1] Author links open overlay panelNikos Chaniotakis et al. (2008) Novel semiconductor materials for the development of chemical sensors and biosensors: A Review, Analytica Chimica Acta. Available at: https://www.sciencedirect.com/science/article/pii/S0003267008005552 (Accessed: 2 August 2025).

[2] Band gap energy (no date) Band Gap Energy - an overview | ScienceDirect Topics. Available at: https://www.sciencedirect.com/topics/engineering/band-gap-energy (Accessed: 2 August 2025).

[3] (No date a) Fermi Dirac distribution function | ELECTRICAL4U. Available at: https://www.electrical4u.com/fermi-dirac-distribution-function/ (Accessed: 3 August 2025).

[4] Author links open overlay panelBen G. Streetman (2007) Semiconductors and transistors, Reference Data for Engineers (Ninth Edition). Available at: https://www.sciencedirect.com/science/article/pii/B9780750672917500200 (Accessed: 5 August 2025).

[5] Nomura, Y. (2024) Density functional theory, Density Functional Theory - an overview | ScienceDirect Topics. Available at: https://www.sciencedirect.com/topics/physics-and-astronomy/density-functional-theory (Accessed: 5 Auguest 2025).

[6] J.P. Perdew (1981) Self-interaction correction to density-functional approximations for many-electron systems | phys. rev. B. Available at: https://journals.aps.org/prb/abstract/10.1103/PhysRevB.23.5048 (Accessed: 5 August 2025).

[7] Righini, G.C. (2019) Solar Cells' Evolution and Perspectives: A short review, Solar Cells and Light Management. Available at: https://www.sciencedirect.com/science/article/pii/B978008102762200001X (Accessed: 6 August 2025).

[8] Materials Project. (2025). Materials Project. [online] Available at: https://next-gen.materialsproject.org/materials/mp-10013?formula=SnS#properties [Accessed 6 Auguest. 2025].

[9] Author links open overlay panelShivani Gohri et al. (2023) Enhancing the efficiency of SNS-based solar cells using a glad technique and CZTSSE layer, Solid State Communications. Available at: https://www.sciencedirect.com/science/article/pii/S0038109823003174 (Accessed: 9 August 2025).